JOTCS B
Journal of the Turkish Chemical Society
Section: B
Chemical Engineering

TURKISH CHEMICAL SOCIETY

SYNTHESIS AND CHARACTERIZATION OF GRAPHENE QUANTUM DOTS FROM DRIED PINE LEAVES

Yunus ÖNAL[1]*, Şifa KIR[2], İlyas DEHRİ[3], Ramazan ESEN[4]

[1]Inonu University, Faculty of Engineering, Department of Chemical Engineering, Malatya, Turkey
[2,3]Cukurova University, Faculty of Science & Letters, Department of Chemistry, Adana, Turkey
[4]Cukurova University, Faculty of Science & Letters, Department of Physics, Adana, Turkey

Abstract: In this study, it was aimed to obtain graphene quantum dots (GQDs) from dried pine leaf (DPL) (peanut pine (*Cedrus libani, Pinus nigra*)). Decomposition temperatures of the dried pine leaf were determined by DTA-TGA analyses in nitrogen atmosphere. DPL was subjected to carbonization in an ash furnace for 6 hours in air, at temperatures of 250, 300, 350 ºC. The materials obtained from the thermal process are characterized using FT-IR, XRD, SEM-EDAX, UV-Vis, and Fluorescence spectrophotometry. When dissolved in deionized water, these materials emit blue fluorescence under UV-A and UV-C excitation. The emission and excitation peaks are very sharp, indicating a homogeneous particle distribution of GQDs in water. When the analysis results were examined, it was observed that the substance was obtained as a result of the carbonization process at 350 ºC for 6 hours and it was compatible with GQDs data in the literature.

Keywords: Graphene Quantum Dots, Pine Leaf, Carbonization.

Submitted: November 08, 2018. **Accepted:** September 20,2019.

Cite this: Önal Y, Kır Ş, Dehri İ, Esen R. SYNTHESIS AND CHARACTERIZATION OF GRAPHENE QUANTUM DOTS FROM DRIED PINE LEAVES. JOTCSB. 2019;2(2):109–20.

***Corresponding author. E-mail:** yunus.onal@inonu.edu.tr.

INTRODUCTION

The exploration of the steam engine, the turning point of the Industry Revolution (1), increased the work of the researchers in the field of carbon in parallel with the increasing demand for coal. Carbon and its allotropes (diamond, graphite, fullerene, buckyball (C60), graphene and carbon nanotube) have become wide spread in the recent material science and applications. Nowadays, nanotechnology-related research has gained speed and new nanomaterials with unique properties such as carbon nanotubes, graphene quantum dots, carbon dots, fluorescent carbon nanotubes, graphene oxides, polymer dots, and nanodiamonds have been included in the literature. Due to the properties of carbon nanomaterials, the uses are increasing day by day; with its unique optical properties, it is gaining importance in the biological applications (5) and oncology (6). As the source for carbon nanomaterials, chitin (7), activated carbon (8), graphite (9), citric acid (10), aspartic acid (11), turmeric (12), glucose (13), lemon peel (14), *Mangifera indica* leaves (15), broccoli (16) etc. raw materials from chemical or natural sources are used. Plants are the perfect source of carbon for the production and biosynthesis of carbon nanomaterial. Carbon nanomaterials can be obtained from the whole parts of the plants, from roots to flowers, from fruits to leaves (17, 18). GQDs which is carbon nanomaterials from the plants are clean, environmentally friendly, and relatively non-toxic. It is possible to obtain

single, double, and multi-layered structures with lateral size graphene layers thinner than 100 nm with diameters ranging within 3-20 nm (19). The GQDs offer unique properties, high transparency, and high surface area, it provides advantages in energy applications (capacitors, lithium ion batteries, and solar cells, etc.)(20). The applications of GQDs in ophthalmic devices, optoelectronics (photodetection, photovoltaics, light-emitting diodes (LEDs), and plasmonics...etc.) are increasing in many fields (21).

GQDs are new materials that have been used in various fields of technology, especially medicine. It can be obtained from every organic structure as well as live and dried leaves of plants. The reason why leaves are preferred is that they carry all the elements of the same chemical structure from nano to macromolecule in the growth stage. When the growth stops, all these structures are present in the leaf and as a result of heat treatment a structural arrangement occurs and they become GQDs structures.

The purpose of this study is to obtain GQDs from dried pine leaf and to determine the properties of the GQDs obtained. For this purpose, the leaves of the peanut pine used, were collected from the Garden of Inonu University in Malatya/Turkey. The connection part of the leaf to the tree trunk was removed by mechanical cleaning. Carbonization method was used for GQDs. The characterization of the obtained GQDs was determined by in situ methods.

MATERIALS AND METHODS

Synthesis of GQDs and Characterization

DTA-TGA analysis was performed in nitrogen atmosphere for dried pine leaf (DPL). In the carbonization process following the decomposition temperature, 250, 300, 350 ^{0}C temperatures were preferred. 100 grams of dried pine leaves were carbonized in air using the ash furnace at the temperatures of 250 ^{0}C (P1); 300 ^{o}C (P2) and 350 °C (P3). Characterization of all samples from the heat treatment was made by FT-IR (Thermo Scientific Nicolet iS10), XRD (Rigaku Miniflex II), Fluorescence spectrophotometer (Perkin Elmer LS 55), CHNS analysis (Thermo Scientific Flash 2000), and SEM (FEI Quanta 650 Model) techniques. UV / VIS (Perkin Elmer Lambda 25) and photoluminescence spectrophotometer (Perkin Elmer LS 55) were used to determine the maximum excitation and emission values of the material and the excitation-related emission activities. Camag UV cabin was used to observe the colors of fluorescence under UV-A and UV-C lamp. Thermal analysis was performed by DTA-TG Mettler Toledo Brand TGA / DSC 3+ system.

RESULTS AND DISCUSSION

DTA-TGA analysis was performed in nitrogen atmosphere of dried pine leaf. The decay temperature was found to be between 130 ^{o}C – 370 ^{0}C (Figure 1).

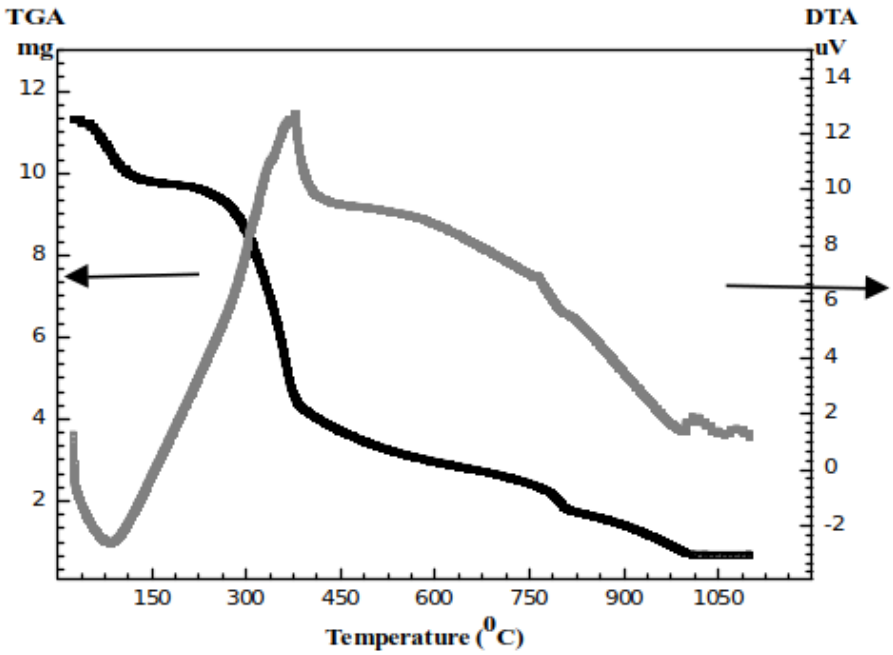

Figure.1. TGA-DTA graph of dried pine leaves (DPL).

When the mass loss-temperature graph was examined, it was observed that for the DPLs which were carbonized for 6 hours at different temperatures, the mass losses increase with the increase of carbonization temperature. There is a mass loss of 44%; 60%; and 90% as a result of the carbonization process at a temperature of 250, 300, and 350 ^{0}C respectively (Figure 2.).

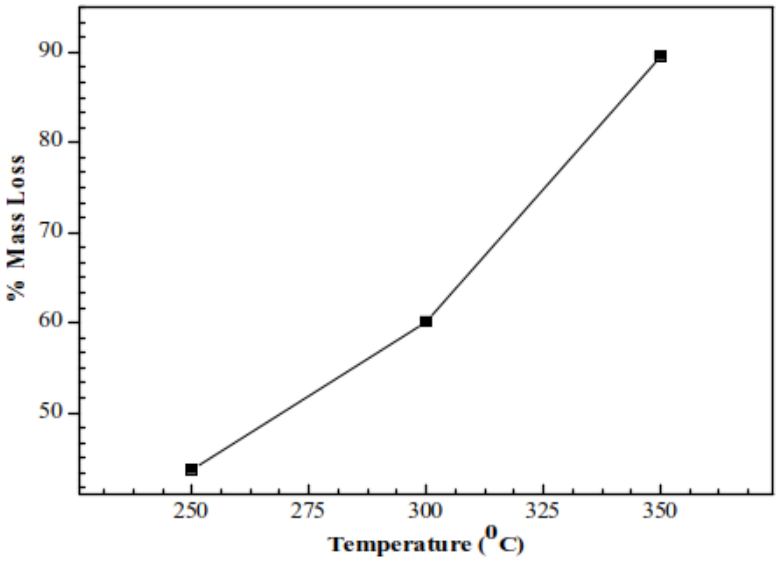

Figure 2. Mass Loss -Temperature Graph.

As a result of the ash determination of DPL, P1, P2, and P3 samples, ash ratio was calculated as 2.93%, 6.08%, 7.84%, and 26.67%, respectively. The results of the original elemental analysis of the substances formed as a result of heat treatment and raw material are given in Table 1. When the results of the elemental analysis calculated by the dry ash free-based method are given in Table 1 in parentheses. When Table 1 is examined, it is seen that the rate of H% in the structure of P1 and P2

decreased; N% and S% increased slightly, while N% and S% increase in the structure of P3; the ratio of C% decreased to 300 ^{0}C and decreased at 350 ^{0}C, parallel to C%, O% decreases to 300 ºC and increases to 350 ^{0}C with the effect of heat treatment . This indicates that a new substance was formed at 350 ^{0}C. In fact, XRD and FT-IR results support this situation.

Table 1. Original elemental analysis results of samples, the values calculated by the dry ashless free-based method are given in parenthesis. (% w/w)

	C%	H%	N%	S%	O% (by difference)
DPL	50.71 (52.24)	6.69 (6.89)	1.58 (1.63)	0.10 (0.10)	40.92 (39.14)
P1	59.98 (63.86)	4.36 (4.64)	2.23 (2.37)	0.10 (0.11)	33.33 (29.01)
P2	61.64 (66.88)	3.46 (3.75)	2.74 (2.97)	0.12 (0.13)	32.04 (26.26)
P3	38.87 (53.01)	1.82 (2.48)	5.08 (6.93)	0.54 (0.74)	53.69 (36.85)

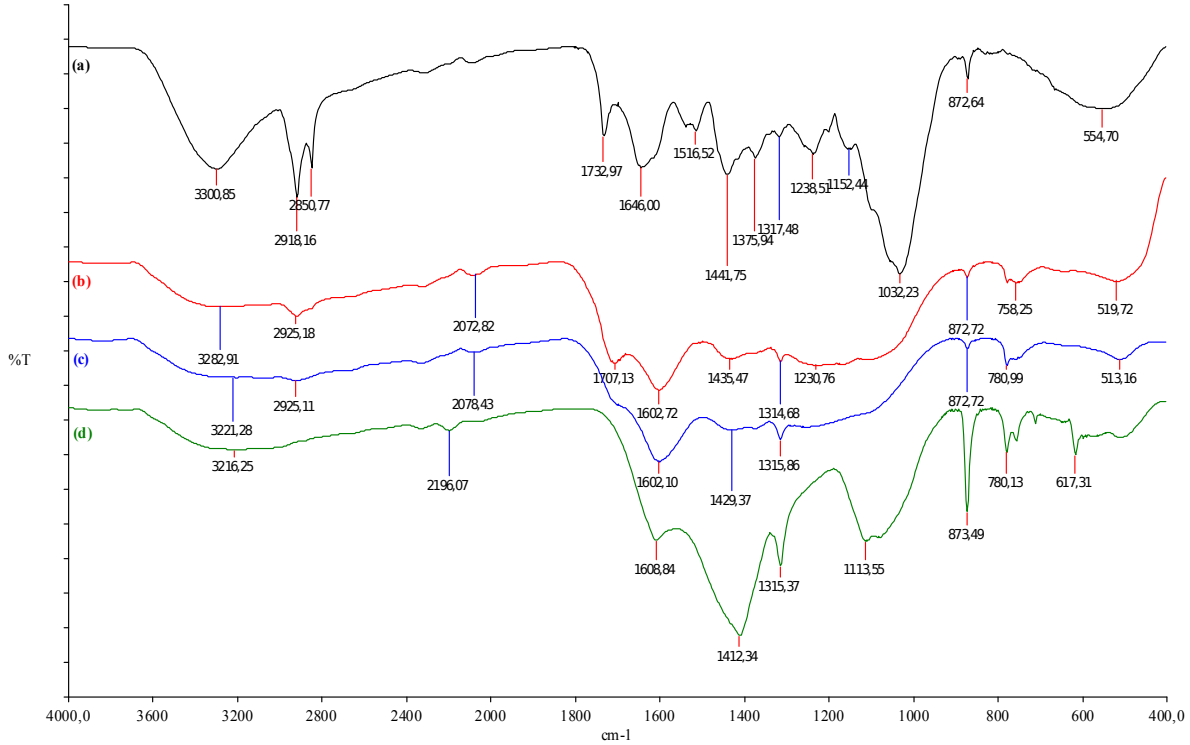

Figure 3. FT-IR spectra of DPL (a), P1 (b), P2 (c), P3 (d).

When FT-IR graphs are examined (Figure 3), it is seen that the DPL is a material with many organic functional groups (Figure 3a). After the carbonization process, aliphatic C-H groups and cellulosic hydroxyl groups leave the matrix. The stretching between 3000-3200 cm^{-1} is clearly seen in the spectrum of dried pine leaf (Figure 3a). The double band at 2850 and 2918 cm^{-1} belongs to the aliphatic C-H stress. The carbonyl band in 1732 cm^{-1} belongs (-C=O) while the band at 1646 cm^{-1} belongs to the structure C=C. The wide and sharp band of 1032 cm^{-1} belongs to M-O-M structures. As the temperature increases, the hydroxyl band disappears due to the structural rearrangement. Similarly, structures with aliphatic C-H bonds appear to be reorganized. The heat treatment results a spectrum, which is similar to the FT-IR spectrum of GQDs structure (Figure 3d) compatible with the literature (15, 23, 24, 27).

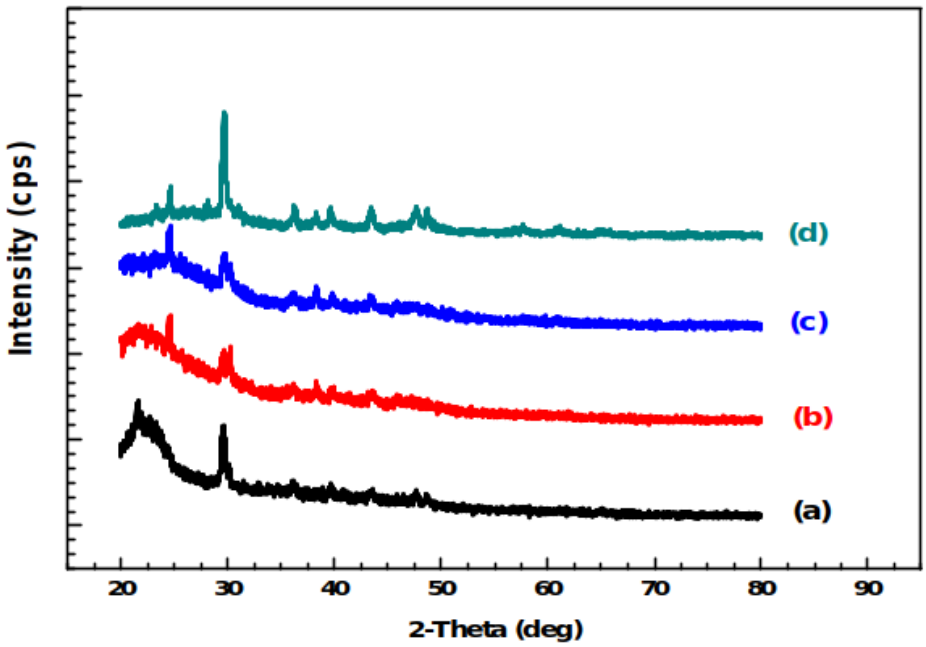

Figure 4. XRD spectrum of DPL (a), P1 (b), P2 (c) P3 (d).

When the XRD results are examined, it is seen that DPL, P1, and P2 materials contain amorphous and crystalline structured regions. The starting DPL contains more amorphous material. After carbonization, the crystalline part increases the reorganization of the system matrix by heating. The sharp peak at 2θ = 24.53 degrees of P3 indicates the presence of graphene particles with a diameter of 3.63 Å (Figure 4). As the temperature increases, the transition from amorphous to polycrystalline structure is observed. As a result of the structure regulation at 350 ^{0}C, the peaks become sharper and symmetrical which indicates pure and better oriented crystallites. In the sample subjected to carbonization at 350 ^{0}C, the diffraction values which were previously at the noise level are noticed at 2θ= 36.13, 38.28, 39.65, 43.38, 47.66, 48.66, 57.51, and 65.20. XRD diffraction data summary is given in Table 2. If the crystallization is continued for longer periods, these peaks may also be assigned. In the literature, most similar organic origin materials also synthesized similar matrices show amorphous structure. In this study, it was observed that the P3 obtained from the DPL, is the crystallites in the sample matrix (25). After carbonization at 350 °C 6 hours $CaCO_3$ grains with sharp peak at 2θ=29.58 forms along a graphene phase with 478 Å size and 2θ= 24.53 (26).

Table 2. X-ray diffraction data summary.

Sample	Main Peaks (2θ)	d(A)	Size(A)	FWHM (deg)	Remarks	Assignment
P3	24.53	3.63	478	0.18	Sharp	Graphene
	29.59	3.01	268	0.320	Sharp	$CaCO_3$

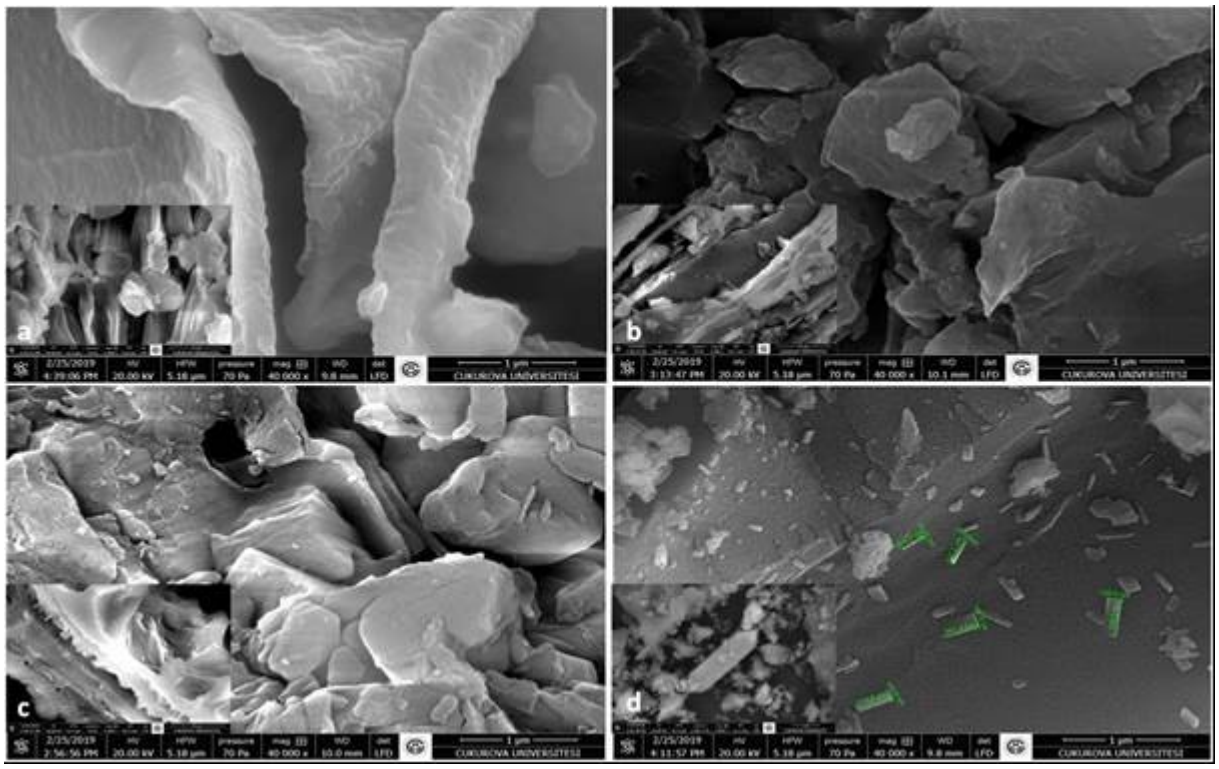

Figure 5. SEM image of DPL (a), P1 (b), P2 (c) P3 (d).

SEM photographs of all samples (a-d) are given in Figure 5. When the SEM image of the DPL is examined, (Figure 5a) it appears to have homogeneous and planar components. It is seen that as a result of heat treatment, cavities form in the structure (Figure 5b), by increasing the temperature, the planar layers begin to form in the structure (Figure 5c). When the SEM graph of P3 is examined, it is seen that a new hexagonal structure appears which is different from P1 and P2 (Figure 5d). When the image of dried pine leaf (Figure 5a) is examined, it is seen that it has a homogeneous structure with small channels. As a result of the heat treatment, it is seen that the channels where the macromolecular structure of the pine leaf is disappeared and new structures are formed due to the structural arrangement as the temperature rises. In fact, mass loss as a result of heat treatment supports this result. Other structures are reorganized from nano to macromolecular structures while small groups of molecules are transitioned to the gas phase. Because of the temperature is not too high, the structural arrangement remains in the crystalline phase (28, 29, 30). The graphene quantum dots are embedded in the carbonized matrice they cannot be seen in SEM studies but they are seen clearly in XRD data. When dissolved in water these GQDs appears in PL (photoluminescence) data which is given in the related section below.

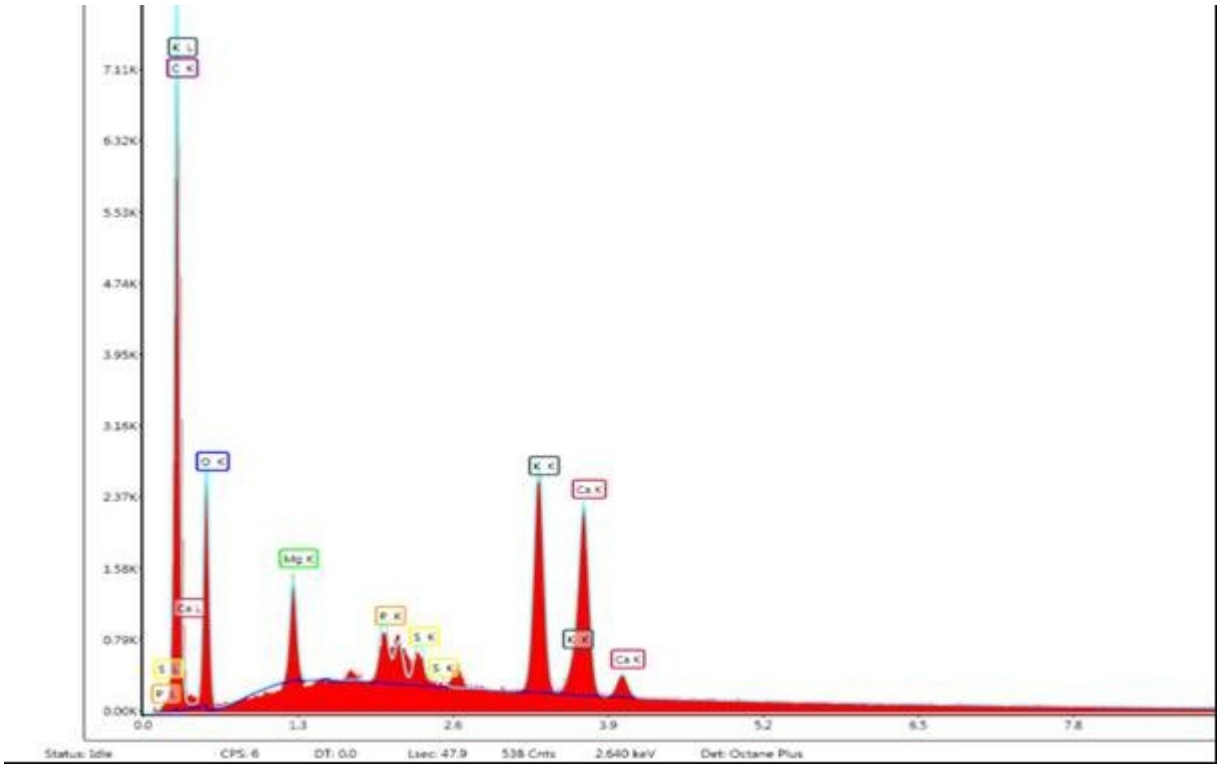

Figure 6. The EDAX graph of P3.

When the EDAX analysis result of the P3 is examined, it is seen that the sample matrix contains mostly C and O elements, along with the other elements Mg, P, S, K, and Ca. When this result is evaluated together with the result of FT-IR, the main structure is organic; the elements of Mg, P, S, K, and Ca may be related to organic functional groups (Figure 6).

For absorbance studies, 1.10^{-3}, 1.10^{-2}, 1.10^{-1}, and 1 g of P3 material and 100 mL of pure water was added to the solution prepared and it was filtered, and it was used for 1 day. The solutions were analyzed using UV-Vis and fluorescence spectrophotometers under UV-A and UV-C lamp illumination. In addition, the results are depicted in Figure 7. In the figure, a very low value of 0.00998 absorbance was observed for the 10^{-3} g / 100 mL sample. For the concentration of 1.10-2 g / 100 mL, 3.6 absorbance value is observed at 333.69 nm wavelength and the absorption peak is narrow and sharp. This indicates that the components that make the fluorescence at this concentration are pure.

A similar result was obtained at a concentration of 1.10^{-1} g / 100 mL. At a concentration of 1 g / 100 mL, the absorbance peak shifted to 340.62 nm and the peak expanded. This can be explained by the amount of water-soluble part of the specimen increased, these components give new absorbance values at different wavelengths. The fluorescence value has decreased significantly. Increased concentration combined with the presence of other components shielded the fluorescence of the UV emitting component.

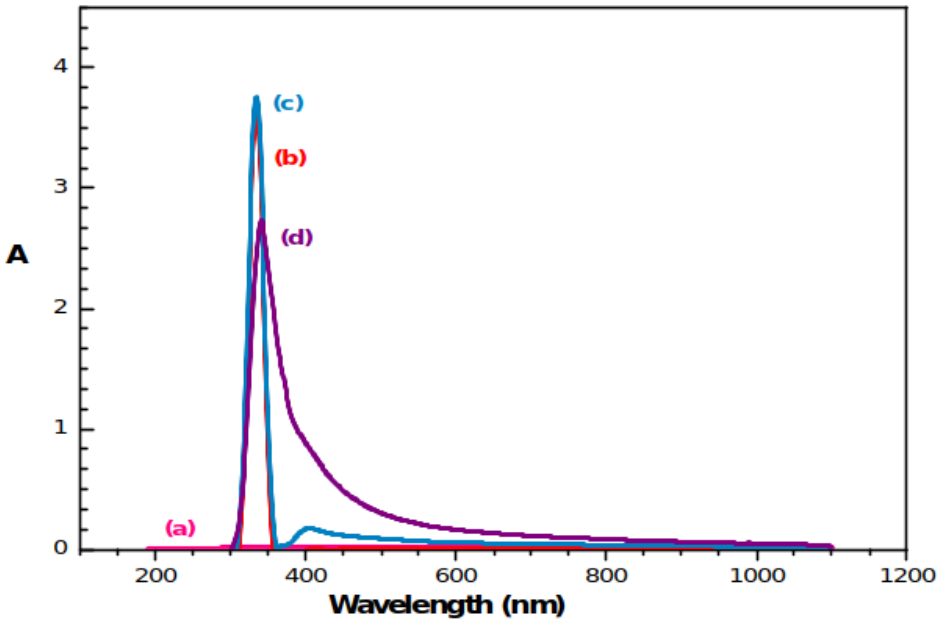

Figure 7. UV-Vis graph of 1.10^{-3} g/100 mL (a), 1.10^{-2} g/100 mL (b), 1.10^{-1} g/100 mL (c), 1 g/100 mL solutions (d).

When the solutions under UV-A and UV-C light were photographed, it was observed that the sample containing 1.10^{-3} g / 100 mL P3 material did not give any fluorescence; other solutions give blue-colored fluorescence, increasing the concentration of solutions increased the fluorescence intensity (Fig. 8).

Figure 8. Left to right, distilled water (1.10^{-3} g, 1.10^{-2} g, 1.10^{-1} g and 1 g of P3 in 100 mL of distilled water) pictured under visible illumination (a), UV-A lamp (360 nm) (b); UV-C lamp (254 nm) (c).

It has been observed that the optical absorption properties of P3 obtained from the carbonization of dried pine leaves have very different properties than the total matrix of material (Figure 7-9). When Table 3 is examined, 1.10^{-2}; 1.10^{-1} and 1 g of P3 solutions gave similar maximum excitation and emission values; the solution of 1.10^{-3} g of P3 was found to be different from the remaining samples. Taking into consideration that the emission and absorption peaks are very sharp, it can be said that they show same absorption wavelength with a measurement error of ± 1 nm. This property attributed to the homogeneity of the samples dissolved in water.

Table 3. Maximum excitation and emission values of prepared solutions.

	Maximum Excitation	**Maximum Emission**
1.10^{-3} g/100 mL	220.1	297.5
1.10^{-2} g/100 mL	537.9	536.6
1.10^{-1} g/100 mL	536.3	534.7
1 g/100 mL	541.9	541.0

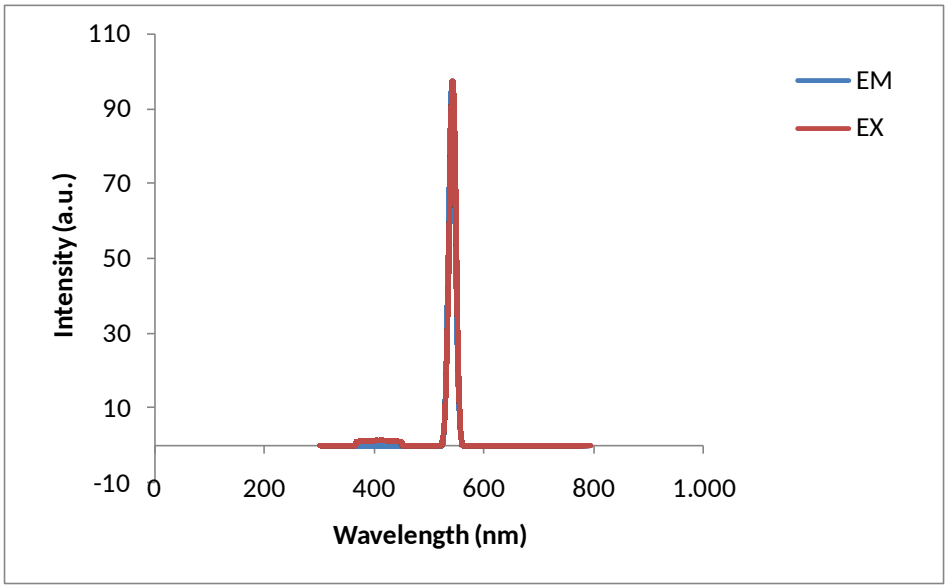

Figure 9. Emission and excitation graph of 1 g / 100 mL of P3 solution. The emission and excitation curves match perfectly so that one obstructs the other in the graph**.**

When the fluorescence analysis results were examined, it was seen that the solution with a concentration of 1.10^{-3} g / 100 mL did not give fluorescence. The emissions of the solutions with 1.10^{-2} g, 1.10^{-1} g, and 1 g of P3 substances show increased fluorescence with the concentration (536.5; 534.5; 541 nm maximum emission values 5.11; 27.91; 97.51 respectively). The graphene quantum dots obtained from dried pine leaves show sharper fluorescence peaks compared to other similar GQDs. This shows that the dimensions of the water-soluble particles have a sharp distribution (1.10^{-3}, 1.10^{-2}, 1.10^{-1}, and 1 g/100 mL distilled water 0.6, 1.3, 1.3, and 1.3 nm). This shows that carbon nanostructures have the same size (homogeneous) distribution in distilled water. The optical PL data is very sharp indicating that structures contain very small number of molecules so widening effects due the size distribution is not observed.

CONCLUSIONS

According to the SEM-EDAX result of raw pine leaf, it was determined that it contains mostly carbon, hydrogen, and oxygen. It is seen that as the temperature increases the mass loss increases as well. However, the elemental analysis show that a high ratio of organic component remains in the environment. As a result of heat treatment, it expected the organic components should decrease in our samples structural reorganization takes place. The FT-IR data also show that many organic components connected to the inorganic components still exist (like $CaCO_3$). After the heat treatment, the P3 sample gave the emission in the UV-A region; it shows that the GQDs in the structure are well crystallized as a crystal structure in nanostructure. When carbonization temperature reaches to 350 ^{0}C a sharp XRD pattern observed at 2θ=29.58 indicating a $CaCO_3$ grain formation with a size of 268 Å. The graphene peak at 2θ=24.53 also observed with 478 Å grain size but with a smaller XRD peak. With this method it is clearly indicated that it can be used as a production method of GQDs.

ACKNOWLEDGEMENT

This study was supported by the unit of Scientific Researches of Çukurova University in Adana, Turkey; Project no: FDK-2016-6191

REFERENCES

1. Külcü R. Sanayi Devriminden 1700 Yıl Önce Yapılmış Erken Bir Keşif: Heron'un Buhar Türbini (Aerolipie). Academia Journal of Social Sciences. 2016;1(2):32-9.

2. Pryzhkova M. V. Concise Review: Carbon Nanotechnology: Perspectives in Stem Cell Research. Stem Cells Translational Medicine. 2013;2:376-83.

3. Jariwala D, Sangwan V. K, Lauhon L. J, Marks T. J, Hersam M. C. et al.Carbon nanomaterials for electronics,

optoelectronics, photovoltaics, and sensing. Chem Soc Rev. 2013;42(7):2824-60.

4. Zhai W, Srikanth N, Kong L. B, Zhou K. et al.Carbon nanomaterials in tribology. Carbon. 2017;119:150-171.

5. Wen J, Xu Y, Li H, Lu A,Sun S. et al. Recent applications of carbon nanomaterials in fluorescence biosensing and bioimaging. Chemical Communications. 2015;51(57):11331–524

6. Mehra N. K, Jain A. K, Nahar M. et al.Carbon nanomaterials in oncology: an expanding horizon. Drug Discovery Today. 2018;23(5):1016-25.

7. Shchipunov Y. A, Khlebnikov O. N, Silant'ev V. E. et al. Carbon Quantum Dots Hydrothermally Synthesized from Chitin. Polymer Science, Ser. B, 2015;57(1):16–22.

8. Qian Z, Chai L, Tang C, Huang Y, Chen J, Feng H. A fluorometric assay for acetylcholinesterase activity and inhibitor screening with carbon quantum dots. Sensors and Actuators B. 2016;222:879–86.

9. Muthurasu A,Ganesh V. et al. Horseradish Peroxidase Enzyme Immobilized Graphene Quantum Dots as Electrochemical Biosensors. Appl Biochem Biotechnol. 2014;174:945–59.

10. Roushani M, Mavaei M, Rajabi H. R. et al. Graphene quantum dots as novel and green nano-materials for thevisible-light-driven photocatalytic degradation of cationic dye. Journal of Molecular Catalysis A: Chemical. 2015;409:102–9.

11. Zhang C, Cui Y, Song L, Liu X, Hu Z. et al. Microwave assisted one-pot synthesis of graphene quantum dots as highly sensitive fluorescent probes for detection of iron ions and pH value. Talanta. 2016;150:54–60.

12. Ahmadian-Fard-Fini S, Salavati-Niasari M, Safardoust-Hojaghan H. et al. Hydrothermal green synthesis and photocatalytic activityof magnetic $CoFe_2O_4$–carbon quantum dots nanocompositeby turmeric precursor. J Mater Sci: Mater Electron. 2017;28:16205–14.

13. Hallaj T, Amjadi M, Manzoori J. L, Shokri R. et al. Chemiluminescence reaction of glucose-derived graphene quantum dots with hypochlorite, and its application to the determination of free chlorine. Microchim Acta. 2015;182:789–96.

14. Chatzimitakos T, Kasouni A, Sygellou L, Avgeropoulos A, Troganis A, Stalikas C. et al. Two of a kind but different: Luminescent carbon quantum dots from Citrus peels for iron and tartrazine sensing and cell imaging. Talanta. 2017;175:305–12.

15. Kumawat M. K, Thakur M, Gurung R. B, Srivastava R. et al. Graphene Quantum Dots from Mangifera indica: Application in Near-Infrared Bioimaging and Intracellular Nanothermometry. ACS Sustainable Chem. Eng. 2017, 5, 1382−91.

16. Arumugam N, Kim J. et al. Synthesis of carbon quantum dots from Broccoli and their ability todetect silver ions. Materials Letters. 2018; 219:37–40.

17. Das R, Bandyopadhyay R, Pramanik P. et al. Carbon quantum dots from natural resource: A review.Materials Today Chemistry. 2018;8:96-109.

18. Zaytseva O, Neumann G. et al. Carbon nanomaterials: production, impact on plant development, agricultural and environmental applications. Chem. Biol. Technol. Agric. 2016;3:17.

19. Benítez-Martínez S, Valcárcel M. et al. Graphene quantum dots as sensor for phenols in olive oil. Sensors and Actuators B. 2014;197:350–7.

20. Bak S, Kim D, Lee H. et al. Graphene quantum dots and their possible energy applications: Areview. Current Applied Physics.2016;16:1192-201.

21. Jin Z, Owour P, Lei S, Ge L. et al. Graphene, graphene quantum dots and their applications in optoelectronics. Current Opinion in Colloid & Interface Science. 2015;20:439–53.

22. Amjadi M, Shokri R, Hallaj T. A new turn-off fluorescence probe based on graphene quantum dots for detection of Au(III) ion. Spectrochimica Acta Part A: Molecular

and Biomolecular Spectroscopy. 2016; 153: 619–24.

23. Habiba K, Makarov V. I, Avalos J, Guinel M. J. F, Weiner B. R, Morell G. et al. Luminescent graphene quantum dots fabricated by pulsed laser synthesis. Carbon. 2013;64:341 –50.

24. Teymourinia H, Salavati-Niasari M, Amiri O, Safardoust-Hojaghan H. et al. Synthesis of graphene quantum dots from corn powder and their application in reduce charge recombination and increase free charge carriers. Journal of Molecular Liquids. 2017; 242: 447–55.

25. Ettefaghi E, Ghobadian B, Rashidi A, Najafi G, Khoshtaghaza M. H, Pourhashem S. et al. Preparation and investigation of the heat transfer properties of a novel nanofluid based on graphene quantum dots. Energy Conversion and Management. 2017;153:215–23.

26. Sekkal W, Zaoui A. et al. Nanoscale analysis of the morphology and surface stability of calcium carbonate polymorphs. Scientıfıc Reports. 2013; 3 : 1587.

27. Das T, Saikiaa B. K, Dekaboruaha H. P, Bordoloia M. et al. Blue-fluorescent and biocompatible carbon dots derived from abundant low quality coals. Journal of Photochemistry & Photobiology, B: Biology. 2019; 195: 1–11.

28. Bedeloğlu A, Taş M, Grafen ve Grafen Üretim Yöntemleri. AKU J. Sci. Eng. 16 2016; 031203: 544-54.

29. Liu X, Yang R, Xu M, et al. Hydrothermal Synthesis of Cellulose Nanocrystal-Grafted-Acrylic Acid Aerogels with Superabsorbent Properties. Polymers. 2018; 10, 1168.

30. Tiyek İ, Dönmez U, Yıldırım B, et. al. Kimyasal yöntem ile indirgenmiş grafen oksit sentezi ve karakterizasyonu. SAÜ Fen Bil Der. 2016; 20. Cilt, 2. Sayı: s. 349-57.